ACS Combinatorial Science

Research Article

pubs.acs.org/acscombsci

# Accelerated Discovery of Thermoelectric Materials: Combinatorial Facility and High-Throughput Measurement of Thermoelectric Power Factor

Jorge García-Cañadas,[†,∥] Nicholas J. E. Adkins,[‡] Stephen McCain,[‡] Bastian Hauptstein,[‡] Ashley Brew,[†] David J. Jarvis,[§] and Gao Min*[,†]

[†]School of Engineering, Cardiff University, The Parade, Cardiff CF24 3AA, United Kingdom

[‡]College of Engineering & Physical Sciences, The University of Birmingham, Edgbaston, Birmingham B15 2TT, United Kingdom

[§]European Space Agency, Keplerlaan 1, PO Box 299, 2200 AG Noordwijk, The Netherlands

**ABSTRACT:** A series of processes have been developed to facilitate the rapid discovery of new promising thermoelectric alloys. A novel combinatorial facility where elements are wire-fed and laser-melted was designed and constructed. Different sample compositions can be achieved by feeding different element wires at specific rates. The composition of all the samples prepared was tested by energy dispersive X-ray spectroscopy (EDS). Then, their thermoelectric properties (power factor) at room temperature were screened in a specially designed new high-throughput setup. After the screening, the thermoelectric properties can be mapped with the possibility of identifying compositional trends. As a proof-of-concept, a promising thermoelectric ternary system, Al−Fe−Ti, has been identified, demonstrating the capability of this accelerated approach.

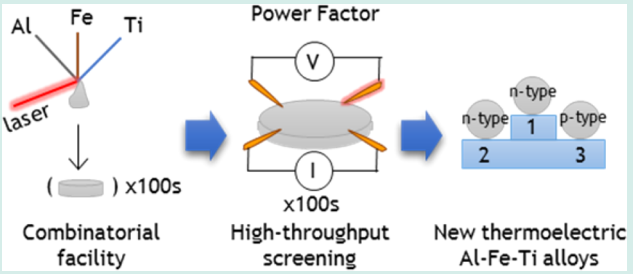


**KEYWORDS:** *high-throughput, thermoelectric materials, laser processing, combinatorial chemistry, power factor*

## INTRODUCTION

Nowadays, there is an increasing demand on power generation. In this respect, thermoelectricity has attracted considerable interest over the past decades due to its ability to directly convert heat into electricity and its application in solid-state refrigeration.[1] Most of the research on developing new materials has been focused on maximizing the dimensionless figure of merit ZT, which relates to the efficiency of the materials. It is defined as $ZT = S^2T/\lambda\rho$, where $S$ is the Seebeck coefficient, $T$ the absolute temperature, $\lambda$ the thermal conductivity, and $\rho$ the electrical resistivity. The power factor, defined as $S^2/\rho$, is also a useful parameter to evaluate thermoelectric performance of materials.

There is a strong demand on high-$ZT$ bulk materials, specially containing environmentally friendly, sustainable and abundant elements.[2] The search for new thermoelectric materials requires huge amounts of sample synthesis and characterization. For this reason, combinatorial approaches are of significant importance for accelerating the discovery of novel materials.[3] Examples of both experimental[4−7] and theoretical approaches[8−11] have been reported in the literature. Employing this approach, a wide number of compounds combining different elements in a wide range of compositions can be synthesized. Then, the relevant properties have to be measured by means of high-throughput facilities, leading to a library of compositional-dependent properties useful to identify promising materials and find out compositional trends.

Here we report an integral combinatorial approach where a vast number of bulk alloy samples have been prepared in a novel combinatorial facility fed by wires of different pure elements. The wires were laser-melted to form the alloys and different compositions were achieved by adapting the feed rate of each wire. The thermoelectric power factor was then screened at room temperature in all the samples using a specially designed high-throughput facility. After an initial screening of hundreds of different samples, a promising ternary system, Al−Fe−Ti was identified.

## EXPERIMENTAL PROCEDURES

**Combinatorial Facility.** This facility is based on the suspended droplet alloying (SDA) concept, which utilizes a laser beam to melt elemental wire feedstock in order to produce a small button of bulk alloy material (see Figure 1). Compositionally different samples can be synthesized by varying the ratio of wire feed rates. The alloying process begins when the aligned wires from each element are fed into the beam path and melt. The melting process initiates the formation of a droplet on the tip of each wire. The elemental droplets grow as new material is fed into them. Because of the proximity of the wires to one another, the droplets join and

**Received:** November 25, 2015
**Revised:** April 28, 2016





DOI: 10.1021/acscombsci.5b00178
ACS Comb. Sci. XXXX, XXX, XXX−XXX

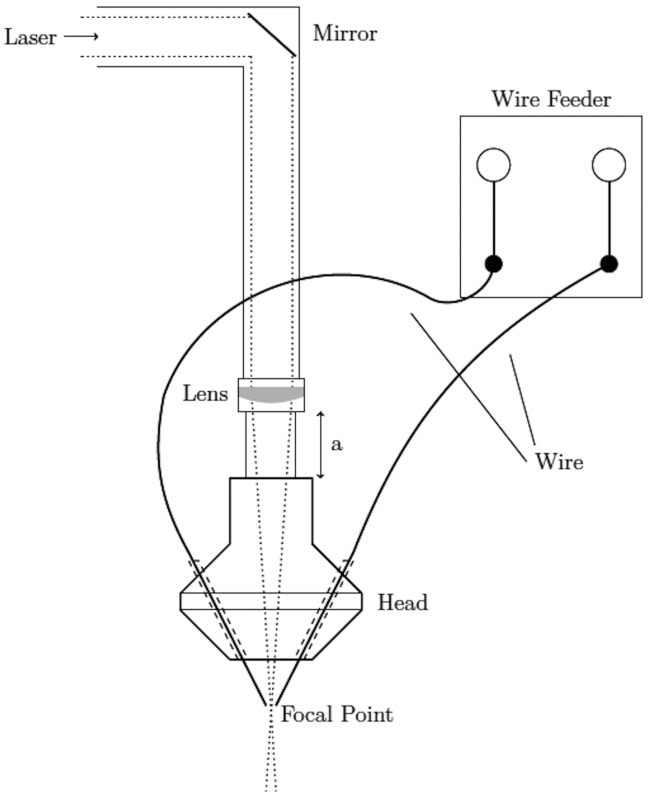


**Figure 1.** Schematic of wire fed suspended droplet alloying process (not to scale).

form a single alloy droplet, which is suspended only by the wires feeding into it. The droplet remains suspended on the tip of the wires due to surface tension. Once the mass of the droplet becomes large enough, the gravity force overcomes the force of surface tension and the droplet detaches from the wires falling onto the substrate. As more of these alloy droplets are deposited, the bottom of the sample begins to freeze. However, it is still possible to maintain a molten pool in the upper region of the sample. This droplet deposition sequence is repeated a number of times until the desired sample height is achieved; at which point the laser and wire feeders are simultaneously stopped. The sample is then allowed to cool under argon shielding gas with a flow rate of 5 L/min. The whole process is performed in an argon filled glovebox with oxygen levels of 30 ppm or less.

The key to the SDA process lies in the ability to mix and alloy relatively small volumes of material while it is in contact with only its constituent parts (the elemental wires). SDA is achieved through precise alignment of the wires with one another in a region where they will intersect the beam path and melt. The wire alignment encourages the elemental droplets to join and mix with one another shortly after their formation. Precise control of the wire feed rates and the 100% capture rate of material allows an alloy with the desired stoichiometry to be produced with a high degree of accuracy.

Feedstock material was purchased from Advent Research Materials (UK). For the case of Al, Fe, and Ti, 1 mm diameter wires with 99.8% purity or higher were used. The substrate material, where the alloy droplets were deposited, was produced from 430-grade stainless steel disc 20 mm in diameter with a thickness of 2 mm. Before alloy synthesis could be commenced some preparatory steps were performed. The wires required to synthesize the thermoelectric alloy were weighed on a four-point balance to ascertain the mass in terms of a linear density (g/m). This allows a target composition in atomic percentage (at. %) to be calculated to a ratio of wire feed rates (mm/min) for individual wires.

The wires required to produce the bulk material were loaded into the wire feeder assemblies, inserted into a copper delivery nozzle and aligned within the beam path. The feed rates (mm/min) required to produce the specific target composition were calculated and entered into the control software for each wire feeder. A substrate was positioned underneath the copper delivery nozzle in the center of the beam path on a *X*,*Y* table. A laser power sufficient to melt the wires at the specified feed rates was selected. The laser beam was then fired in continuous wave mode and the wire feeders were activated. Samples are typically produced in 2 min.

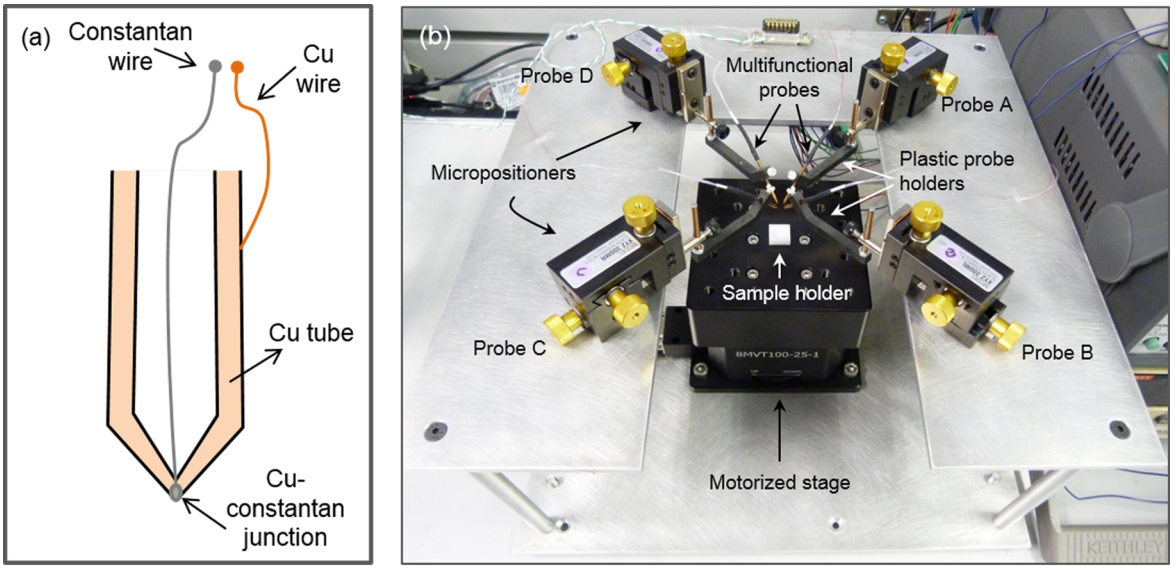


**Figure 2.** (a) Scheme of the components of a multifunctional probe. (b) Picture of the power factor screening facility.



DOI: 10.1021/acscombsci.5b00178
*ACS Comb. Sci.* XXXX, XXX, XXX−XXX

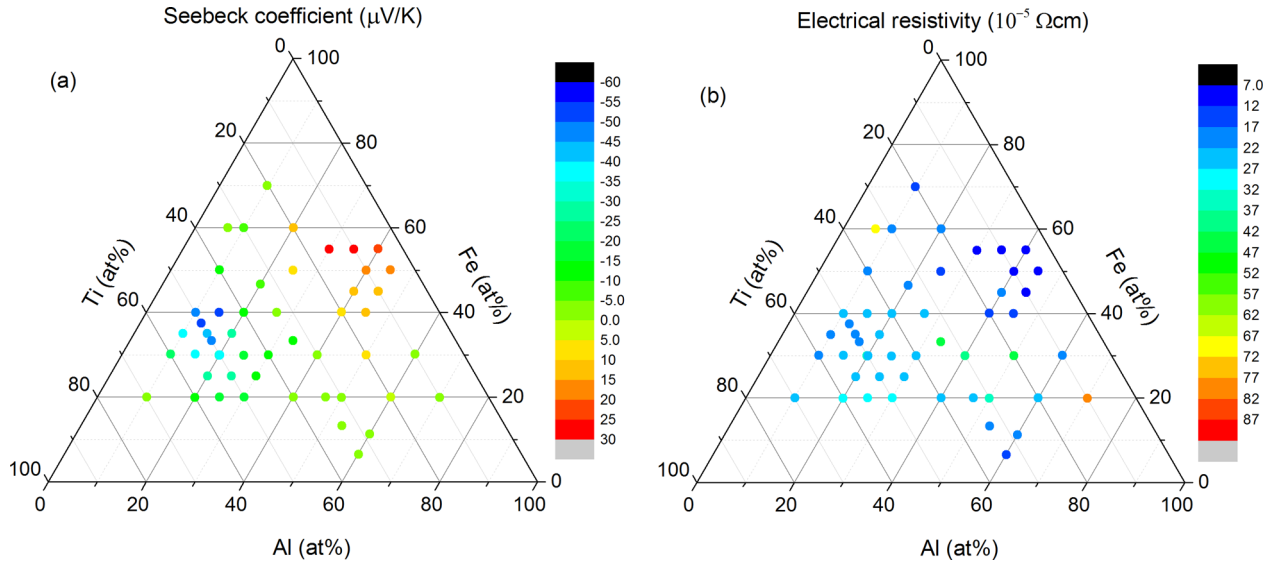


**Figure 3.** Thermoelectric screening of the Al−Fe−Ti ternary alloys: (a) the Seebeck coefficient and (b) electrical conductivity.

For the screening of the thermoelectric properties the samples were cut to a 1−2 mm thick disc perpendicular to the build direction using an AgieCharmilles Cut 20 EDM. This disc was then ground and polished. Discs diameter varied from 6 to 15 mm. Sample composition was confirmed using a Hitachi TM3000 Desktop Scanning Electron Microscope (SEM) with Bruker XFlash 4010 Energy Dispersive X-ray Spectroscopy (EDS) detector in conjunction with Bruker Quantax Esprit 1.9 software. An agreement of ±2% respect to the compositions from the feed was found. No compositional gradients were identified from EDS measurements performed at different surface points on the sample discs Phase identification was performed in selected samples by X-ray diffraction (XRD) using a Phillips PW1710 Automated Powder Diffractometer with copper (Cu K$\alpha$) radiation at 35 kV and 40 mA. The diffractometer was controlled with PW1877 APD version 3.6 computer software and initial phase identification was performed using PW1876 PC-Identift version 1.0b software. XRD samples were prepared by grinding the discs with a pestle and mortar to a powder and packing them into an aluminum holder.

**High-Throughput Power Factor Measurement Facility.** The measurement of the power factor involves the determination of both Seebeck coefficient and electrical resistivity. Unlike thermal conductivity, the power factor can be measured quicker and has been chosen as the main indicator for the initial screening of the thermoelectric performance. Examples of high-throughput tools for the measurement of power factor can be found in the literature, most of them focused on thin films.[5,7,12,13] Although it can also be used for thin films, the facility we developed for the screening of the power factor was designed for bulk samples. The details of the apparatus have been recently reported.[14] As a summary, the equipment measures the electrical resistivity using the Van der Pauw method[15] and the Seebeck coefficient is measured by means of a hot probe. The key aspect of the facility is the use of 4 multifunctional probes. Each multifunctional probe consists of a Cu tube with a constantan wire welded right at the tip, forming a T-type thermocouple as shown in Figure 2a. In this way, the temperature can be measured right at each probe tip and the Cu part can be used to provide electrical contacts for the flow of current and the measurement of voltages.

For the measurement the sample was first placed on a sample holder fixed on a motorized stage (Figure 2b). Then, the stage was lifted and the 4 multifunctional probes were contacted at the edges of the sample, as required by the Van der Pauw method. Inside probe A, a heater coil was installed to set its temperature ∼3 K above room temperature to allow Seebeck coefficient measurements. By consecutively measuring the temperatures at the tips of probes A ($T_A$) and D ($T_D$), and the open-circuit voltage difference ($\Delta V$) across them through their Cu wires, the Seebeck coefficient of the sample was calculated as $S = \Delta V/(T_A - T_D) + S_{Cu}$ ($S_{Cu}$ is the Seebeck coefficient of the Cu used in the multifunctional probes[14]). The electrical resistivity was measured directly afterward (keeping probe A hot) by applying current across two adjacent probes and measuring the induced voltage difference at the other two. This was performed varying the polarity and alternating the different pairs of probes to obtain the required number of measurements to obtain the sheet resistance $R_s$ and then the electrical conductivity $\rho = R_s d$ ($d$ is the thickness of the sample[14]). Finally, the stage was moved down to its original position and the sample removed to allow the positioning of the next one. All the measurements, automated and controlled by a computer, were performed in around 20 s. To our knowledge, this is the fastest power factor measurement reported so far. By adding the time required to place the sample and contact the 4 multifunctional probes by means of the micropositioners, a total time of 1 to 2 min could be expected per sample.

## RESULTS AND DISCUSSION

Around 500 samples comprising single elements, binary and ternary alloys were initially synthesized and their power factor screened. From the analysis of the library of results a promising ternary alloy system formed by Al−Fe−Ti was identified. The ternary diagrams showing the Seebeck coefficient and electrical resistivity data are shown in Figure 3. The most negative Seebeck coefficient value measured was −57 $\mu$V/K, corresponding to the $Al_{12.5}Fe_{37.5}Ti_{50}$ composition (Figure 3a). Not very far values were observed for close compositions.


DOI: 10.1021/acscombsci.5b00178
ACS Comb. Sci. XXXX, XXX, XXX−XXX

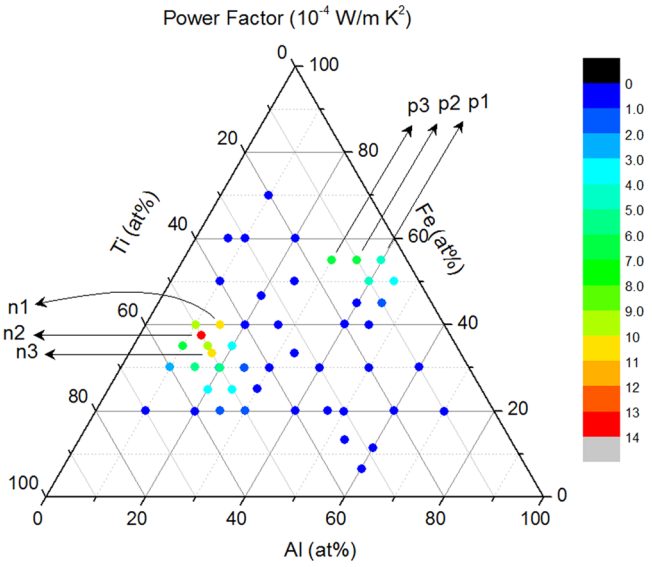


**Figure 4.** Results of thermoelectric screening of the power factor of the Al−Fe−Ti ternary system. Samples n1−n3 and p1−p3 are the best *n*- and *p*-type samples identified, respectively.

Interestingly, samples with positive Seebeck coefficient could be found when Ti content is decreased below 30%, with several compositions showing around 27 $\mu$V/K. The lower Ti content of the alloys seems to be the most significant parameter affecting the transition from negative to positive Seebeck coefficients, which might cause the decrease of the mean free path with the electron energy.[16] It should be noted that the existence of both positive and negative values of Seebeck coefficient is highly beneficial, since both are required when the materials are assembled to form a device and this characteristic is not always present in thermoelectric bulk materials.

The electrical resistivity values are shown in Figure 3b. They lie in the order of $10^{-4}$ Ω cm, an order of magnitude lower than well-established materials such as $Bi_2Te_3$. Slightly lower values were observed in the area of positive Seebeck coefficients (lower Ti content). The results of the power factor are shown in Figure 4. The highest power factor ($13.3 \times 10^{-4}$ W/m K$^2$) was observed in $Al_{12.5}Fe_{37.5}Ti_{50}$, corresponding to the composition of the most negative value of the Seebeck coefficient mentioned above. The highest power factor observed for positive Seebeck coefficient samples ($7.0 \times 10^{-4}$ W/m K$^2$) was obtained from $Al_{30}Fe_{55}Ti_{15}$. It can be seen that the large power factors are located around the above-mentioned compositions, and away from these compositions, the power factors were much lower.

Although the screened values of the power factor are lower than $Bi_2Te_3$ based alloys (typically around $30 \times 10^{-4}$ W/m K$^2$), they are comparable to the room temperature values of established high temperature thermoelectric materials, such as skutterudites and half heuslers. It should be noted that Al, Fe, and Ti are nontoxic and among the most earth-abundant elements of the periodic table.[2] Among a wide range of thermoelectric materials only silicides and oxides exhibit similar abundance. The thermal conductivity of the best samples was also measured to be in the range of 3−9 W/m K. Clearly, the

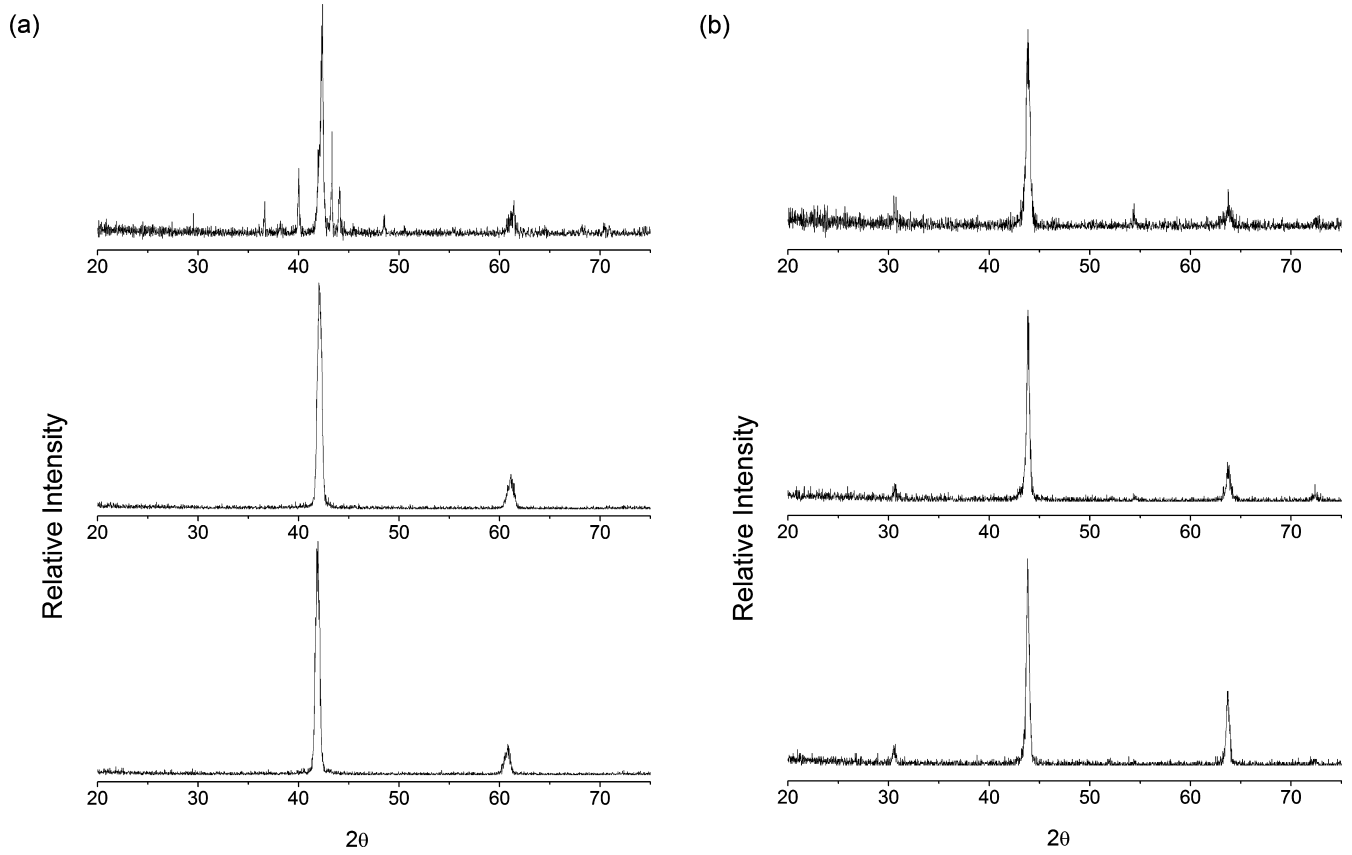


**Figure 5.** (a) From top to bottom, XRD of n1, n2, and n3 samples (see Figure 4). (b) From top to bottom, XRD of p1, p2, and p3 samples (see Figure 4).



DOI: 10.1021/acscombsci.5b00178
ACS Comb. Sci. XXXX, XXX, XXX−XXX

Al−Fe−Ti system shows promising thermoelectric properties, which is being further investigated.

XRD of samples with promising properties were carried out to identify the crystalline phases present and to compare them to those expected from literature phase diagrams. Figure 5a shows the results of materials that exhibit n-type behavior, whereas Figure 5b shows p-type samples. When comparing the compositions of the 3 n-type materials to the isothermal sections for this alloy system,[17] they are expected to exhibit a base centered cubic (bcc) phase but may also contain the hexagonal Laves (C14) phase. The presence of two peaks at 42° and 61° in the XRD of n2 and n3 samples (bottom and middle, Figure 5a) shows that only the bcc phase is present in these materials and they exhibit A2 ordering. As there are no peaks to imply B2 order, no further atomic ordering in the phase of these materials can be concluded.[18] Material n1 (top, Figure 5a) contains an A2 bcc phase along with a minority C14 hexagonal phase, signified by diffraction peaks which were not previously assigned to the bcc A2 phase. The presence of two phases in this material is expected by considering its position on the isothermal sections of this ternary system: it is located between the cubic and hexagonal stable phases.[17] The three p-type materials have compositions which are expected to crystallize to form bcc structures, as shown from the isothermal sections.[17] Either a disordered A2, a partially ordered B2 or full Heusler bcc phase with all atoms in defined positions should be expected. Our XRD results in Figure 5b imply that all three p-type materials exhibit only a bcc phase. The peaks at 44° and 64° indicate that this phase presents at least A2 ordering, peaks at 30.5°, 54.5°, and 72.5° show that B2 ordering is present and no peaks for the $L2_1$ full Heusler phase are observed.[18] The above results indicate good correlation between the phases identified and those expected from reported isothermal sections.

The identification of the Al−Fe−Ti system as a promising thermoelectric candidate was a surprise and the discovery of both n-and p-type existing in this alloy system was completely unexpected. These results demonstrate the validity of using the above-reported high-throughput techniques as an effective approach for accelerated discovery of thermoelectric materials. They can offer the capability of high-speed discovery of advanced materials, particularly among a large number of ternary or quaternary intermetallic compounds.

## CONCLUSIONS

An integrated combinatorial approach has been developed for accelerated discovery of thermoelectric materials based on a laser melting technique for materials preparation and a multifunctional-probe facility for thermoelectric characterization. Hundreds of samples have been synthesized and their room temperature power factors were characterized. This initial work has led to the identification of a promising ternary system, Al−Fe−Ti, which exhibits a maximum power factor of $13.3 \times 10^{-4}$ W/m $K^2$. This value is comparable to those of the current high temperature thermoelectric materials. In addition, they are abundant and nontoxic and both n- and p-type exist. The discovery of high power factor in Al−Fe−Ti system was unexpected, which demonstrate the validity and effectiveness of the high-throughput approach/techniques (reported in this paper) for the development of advanced materials.

## AUTHOR INFORMATION


### Corresponding Author

*E-mail: min@cardiff.ac.uk.

### Present Address

[‖]J.G.-C.: Department of Industrial Systems Engineering and Design, Universitat Jaume I, Campus del Riu Sec, 12071 Castellon, Spain.


### Author Contributions

The manuscript was written through contributions of all authors. All authors have given approval to the final version of the manuscript.


### Funding

The authors wish to acknowledge financial support from the Accelerated Metallurgy Project, which is cofunded by the European Commission in the seventh Framework Programme (contract NMP4-LA-2011-263206), by the European Space Agency and by the individual partner organizations.


### Notes

The authors declare no competing financial interest.

## ACKNOWLEDGMENTS


Granta Design Ltd. is acknowledged for providing the database and results library.


## REFERENCES


(1) Martín-González, M.; Caballero-Calero, O.; Díaz-Chao, P. Nanoengineering Thermoelectrics for 21st Century: Energy Harvesting and Other Trends in the Field. *Renewable Sustainable Energy Rev.* **2013**, *24* (0), 288−305.

(2) Gaultois, M. W.; Sparks, T. D.; Borg, C. K. H.; Seshadri, R.; Bonificio, W. D.; Clarke, D. R. Data-Driven Review of Thermoelectric Materials: Performance and Resource Considerations. *Chem. Mater.* **2013**, *25* (15), 2911−2920.

(3) Curtarolo, S.; Hart, G. L. W.; Nardelli, M. B.; Mingo, N.; Sanvito, S.; Levy, O. The High-Throughput Highway to Computational Materials Design. *Nat. Mater.* **2013**, *12* (3), 191−201.

(4) Funahashi, R.; Urata, S.; Kitawaki, M. Exploration of N-Type Oxides by High Throughput Screening. *Appl. Surf. Sci.* **2004**, *223* (1−3), 44−48.

(5) Otani, M.; Lowhorn, N. D.; Schenck, P. K.; Wong-Ng, W.; Green, M. L.; Itaka, K.; Koinuma, H. A High-Throughput Thermoelectric Power-Factor Screening Tool for Rapid Construction of Thermoelectric Property Diagrams. *Appl. Phys. Lett.* **2007**, *91* (13), 132102.

(6) Watanabe, M.; Kita, T.; Fukumura, T.; Ohtomo, a.; Ueno, K.; Kawasaki, M. Combinatorial Synthesis and High Throughput Evaluation of Thermoelectric Power Factor in Mg-Si-Ge Ternary Compounds. *Appl. Surf. Sci.* **2007**, *254* (3), 777−780.

(7) Potyrailo, R.; Rajan, K.; Stowe, K.; Takeuchi, I.; Chisholm, B.; Lam, H. Combinatorial and High-Throughput Screening of Materials Libraries: Review of State of the Art. *ACS Comb. Sci* **2011**, 579−633.

(8) Hautier, G.; Jain, A.; Ong, S. P. From the Computer to the Laboratory: Materials Discovery and Design Using First-Principles Calculations. *J. Mater. Sci.* **2012**, *47* (21), 7317−7340.

(9) Bera, C.; Jacob, S.; Opahle, I.; Gunda, N. S. H.; Chmielowski, R.; Dennler, G.; Madsen, G. K. H. Integrated Computational Materials Discovery of Silver Doped Tin Sulfide as a Thermoelectric Material. *Phys. Chem. Chem. Phys.* **2014**, *16*, 19894−19899.

(10) Carrete, J.; Li, W.; Mingo, N.; Wang, S.; Curtarolo, S. Finding Unprecedentedly Low-Thermal-Conductivity Half-Heusler Semiconductors via High-Throughput Materials Modeling. *Phys. Rev. X* **2014**, *4*, 011019.

(11) Yan, J.; Gorai, P.; Ortiz, B.; Miller, S.; Barnett, S. a.; Mason, T.; Stevanović, V.; Toberer, E. S. Material Descriptors for Predicting Thermoelectric Performance. *Energy Environ. Sci.* **2015**, *8*, 983−994.




DOI: 10.1021/acscombsci.5b00178
*ACS Comb. Sci.* XXXX, XXX, XXX−XXX

(12) Yan, Y. G.; Martin, J.; Wong-Ng, W.; Green, M.; Tang, X. F. A Temperature Dependent Screening Tool for High Throughput Thermoelectric Characterization of Combinatorial Films. *Rev. Sci. Instrum.* **2013**, *84* (11), 115110.
(13) Watanabe, M.; Kita, T.; Fukumura, T.; Ohtomo, A.; Ueno, K.; Kawasaki, M. High-Throughput Screening for Combinatorial Thin-Film Library of Thermoelectric Materials. *J. Comb. Chem.* **2008**, *10* (2), 175−178.
(14) García-Cañadas, J.; Min, G. Multifunctional Probes for High-Throughput Measurement of Seebeck Coefficient and Electrical Conductivity at Room Temperature. *Rev. Sci. Instrum.* **2014**, *85* (4), 043906.
(15) Van der Pauw, L. J. A Method of Measuring Specific Resistivity and Hall Effect of Discs of Arbitrary Shape. *Philips Res. Reports* **1958**, *13* (1), 1−9.
(16) Kasap, S. O. *Thermoelectric Effects in Metals: Thermocouples*; University of Saskatchewan: Saskatchewan, Canada, 2001
(17) Palm, M.; Lacaze, J. Assessment of the Al−Fe−Ti System. *Intermetallics* **2006**, *14* (10−11), 1291−1303.
(18) Yin, M.; Hasier, J.; Nash, P. A Review of Phase Equilibria in Heusler Alloy Systems Containing Fe, Co or Ni. *J. Mater. Sci.* **2016**, *51* (1), 50−70.


DOI: 10.1021/acscombsci.5b00178
*ACS Comb. Sci.* XXXX, XXX, XXX−XXX